SUPPORTING INFORMATION

60 K wide hysteresis embracing room temperature in a fluorescent Fe^{II} spin transition complex

Maksym Seredyuk[a], Kateryna Znovjyak[a], Francisco Javier Valverde-Muñoz[b,g], M. Carmen Muñoz[c], Teresa Delgado[d,e], Ivan da Silva[f], José Antonio Real[g]

[a]Department of Chemistry, Taras Shevchenko National University of Kyiv, Kyiv 01601, Ukraine
[b]Departament Matériaux et Lumière Institut de Physique de Rennes Université de Rennes 1, UMR UR1-CNRS 6251, 35000 Rennes (France); orcid.org/0000-0003-3578-5445.
[c]Departamento de Física Aplicada, Universitat Politècnica de València, Camino de Vera s/n, E-46022 Valencia, Spain; orcid.org/0000-0003-2630-3897.
[d]PSL University, Chimie ParisTech – CNRS, Institut de Recherche de Chimie Paris, 11 Rue Pierre et Marie Curie, Paris 75005, France.
[e]Pharmacy Department, CEU Cardenal Herrera University, CEU Universities C/Ramón y Cajal s/n, Alfara del Patriarca, 46115 Valencia, Spain; orcid.org/0000-0002-3155-8889.
[f]ISIS Neutron Facility, STFC Rutherford Appleton Laboratory, Chilton, Oxfordshire, OX11 0QX, UK; orcid.org/0000-0002-4472-9675.
[g]Instituto de Ciencia Molecular, Departamento de Química Inorgánica, Universidad de Valencia, 46980 Paterna, Valencia, Spain. ; orcid.org/0000-0002-2302-561X; E-mail: jose.a.real@uv.es

Contents

Table S1. Crystallographic information of **4Cl**·2MeOH.

Temperature/K	**291(1)**
Empirical formula	$C_{34}H_{28}Cl_2FeN_{12}O_2$
Formula weight	763.43
Crystal system	orthorhombic
Space group	*Pbcn*
Crystal size/mm^3	0.08 × 0.06 × 0.05
a/Å	12.9255(9)
b/Å	10.1011(8)
c/Å	27.808(3)
V/Å^3	3630.6(5)
Z	4
ρ_{calc} g/cm^3	1.397
μ/mm^{-1}	0.612
F(000)	1568
Reflections collected	3190
Independent reflections	1185
Goodness-of-fit on F^2	0.968
Final R indexes [I>=2σ (I)]	R = 0.0745,
Final R indexes [all data]	R = 0.2082,
Largest diff. peak/hole / e Å^{-3}	0.338/-0.404

Table S2. Short intermolecular contacts for compound **4Cl**·2MeOH.

4Cl·2MeOH	**Length**	**Length-VdW**	**Symm. op. 1**	**Symm. op. 2**
H2···C15	2.790	-0.140	x,y,z	-x,-1+y,1.5-z
H1···N6	2.362	-0.388	-x,y,1.5-z	-1/2-x,-1/2+y,z
H7···C1	2.763	-0.137	-x,y,1.5-z	-1/2-x,-1/2+y,z
H18···N5	1.832	-0.918	x,y,z	x,y,z
N5···O12	2.794	-0.276	x,y,z	x,y,z
C10···C18	2.895	-0.005	x,y,z	x,y,z
H17A···C3	2.869	-0.031	-x,y,1.5-z	x,y,z
H3···O1	2.401	-0.319	x,y,z	1/2+x,1/2+y,1.5-z
H5···O1	2.485	-0.235	x,y,z	1/2+x,1/2+y,1.5-z
C15···C2	3.686	0.286	x,y,z	-x,-1+y,1.5-z
C6···C2	3.624	0.224	-x,y,1.5-z	-1/2+x,-1/2+y,1.5-z
C6···C3	3.469	0.069	-x,y,1.5-z	-1/2+y,1.5-z
C7···C3	3.557	0.157	-x,y,1.5-z	-1/2+x,-1/2+y
C7···C1	3.661	0.261	-x,y,1.5-z	-1/2-x,-1/2+y,z
C9···C5	3.688	0.288	-x,y,1.5-z	-1/2+x,-1/2+y,1.5-z
C12···C9	3.605	0.205	-x,y,1.5-z	-1/2+x,-1/2+y,1.5-z
C3···C17	3.687	0.287	-x,y,1.5-z	x,y,z
C15···C17	3.669	0.269	x,y,z	-x,-y,1-z

Table S3. Crystallographic and Rietveld refinement information of **4Cl** in the LS and HS states.

	4Cl(LS)	**4Cl**(HS)
Temperature (K)	100	298
Space group	*Pbcn*	
a (Å)	13.04002(18)	13.31794(11)
b (Å)	10.50377(19)	9.10907(8)
c (Å)	21.4355(3)	24.7285(3)
V (Å^3)	2936.00(8)	2999.91(5)
Z	4	
D_c (mg cm^{-3})	1.5821	1.5484
Radiation Type	Synchrotron	
Diffractometer	I11 at Diamond Light Source, UK	
Data collection mode	Transmission	
Wavelength (Å)	0.826844	
R_p (%)	4.57	4.70
R_{wp} (%)	5.92	5.95
R_{exp} (%)	4.24	3.17
Goodness-of-fit	1.40	1.88
R_B (%)	1.90	2.80

Table S4. Short intermolecular contacts for compound **4Cl** in the HS and LS state.

4Cl (HS)	**Length**	**Length-VdW**	**Symm. op. 1**	**Symm. op. 2**
H2···C11	2.846	-0.054	x,y,z	1-x,-1+y,1.5-z
H2···C16	2.736	-0.164	x,y,z	1-x,-1+y,1.5-z
H2···C15	2.845	-0.055	x,y,z	1-x,-1+y,1.5-z
H3···N5	2.401	-0.349	1-x,y,1.5-z	1/2-x,-1/2+y,z

4Cl (LS)	**Length**	**Length-VdW**	**Symm. op. 1**	**Symm. op. 2**
H2···C15	2.790	-0.110	x,y,z	1-x,-1+y,1.5-z
H2···C14	2.612	-0.288	x,y,z	1-x,-1+y,1.5-z
H2···C13	2.664	-0.236	x,y,z	1-x,-1+y,1.5-z
H2···C12	2.868	-0.032	x,y,z	1-x,-1+y,1.5-z
H1···Cl	2.802	-0.148	x,y,z	x,2-y,-1/2+z
C3···H12	2.549	-0.351	1-x,y,1.5-z	1/2-x,-1/2+y,z
H3···N5	2.480	-0.270	1-x,y,1.5-z	1/2-x,-1/2+y,z
H3···H12	2.290	-0.110	1-x,y,1.5-z	1/2-x,-1/2+y,z
H5···N5	2.685	-0.065	1-x,y,1.5-z	1/2-x,-1/2+y,z

Table S5. The full color-coded interaction mappings of a central reference molecule with nearest neighbors of **4Cl** and the contributions to the total energy in both spin states as calculated by DTF B3LYP/6-31G(d,p) method.

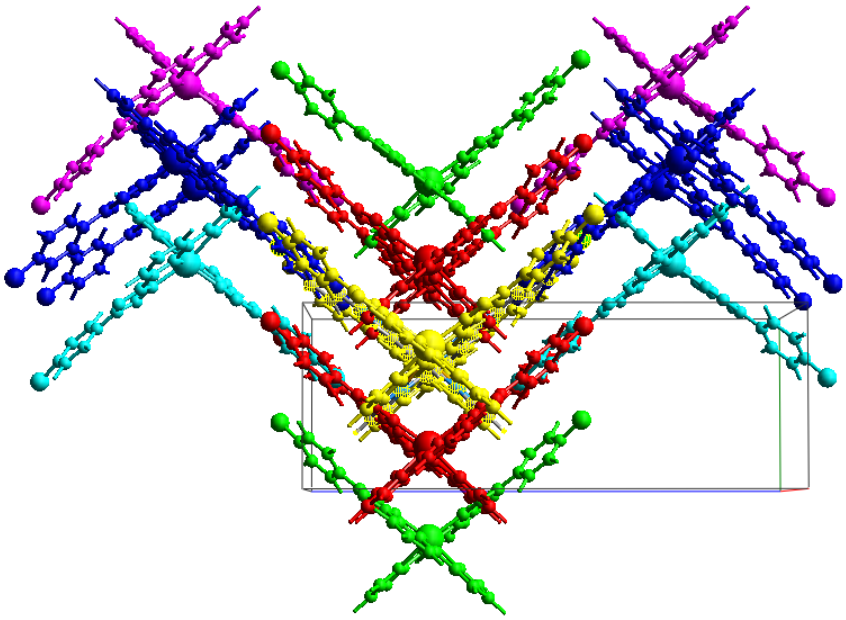

	Symmetry operation	Spin state	R, Å	**ΔR**	*E*, kJ mol^{-1}					
					Electrostatic	Polarization	Dispersion	Exchange-repulsion	**Total**	**Δ*E*(total)(HS – LS)**
	x+1/2, y+1/2, -z+1/2	LS	8.37	**-0.30**	-30.9	-15.5	-75.9	67.6	-68.4	**-7,90**
		HS	8.07		-33.1	-15.6	-81.9	67.3	-76.3	
	x, y, z	LS	13.04	**0.28**	11.3	-1.2	-4.1	0.0	7.5	**-2,30**
		HS	13.32		10.7	-1.5	-5.7	0.0	5.2	
	x, y, z	LS	10.50	**-1.39**	-24.7	-6.0	-43.0	47.4	-38.7	**-4,50**
		HS	9.11		-20.1	-5.6	-45.0	34.5	-43.2	
	-x, -y, -z	LS	10.96	**1.57**	-22.2	-12.3	-79.0	65.5	-60.9	**-0,90**
		HS	12.53		7.4	-10.7	-70.9	0.0	-61.8	
	-x+1/2, -y+1/2, z+1/2	LS	14.63	**0.87**	-9.1	-1.7	-14.5	0.0	-23.5	**6,70**
		HS	15.50		-5.6	-1.1	-11.5	0.0	-16.8	

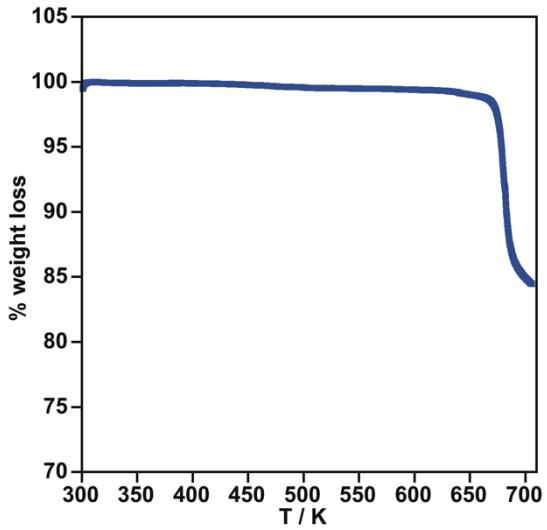

Figure S1. Thermal stability of **4Cl**.

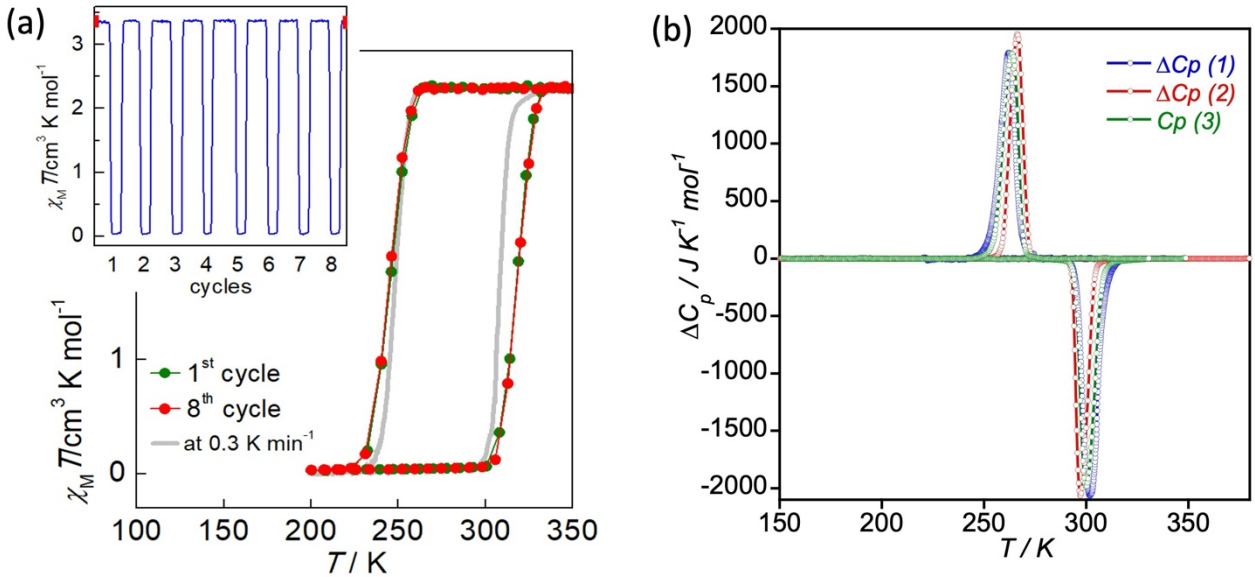

Figure S2. Stability of the **4Cl** spin transition: (a) $\chi_M T$ vs T plots at 4K/min (8 cycles) compared with the 0.3 K/min one (grey line) represented as reference. (d) Three cycles of ΔCp vs T.

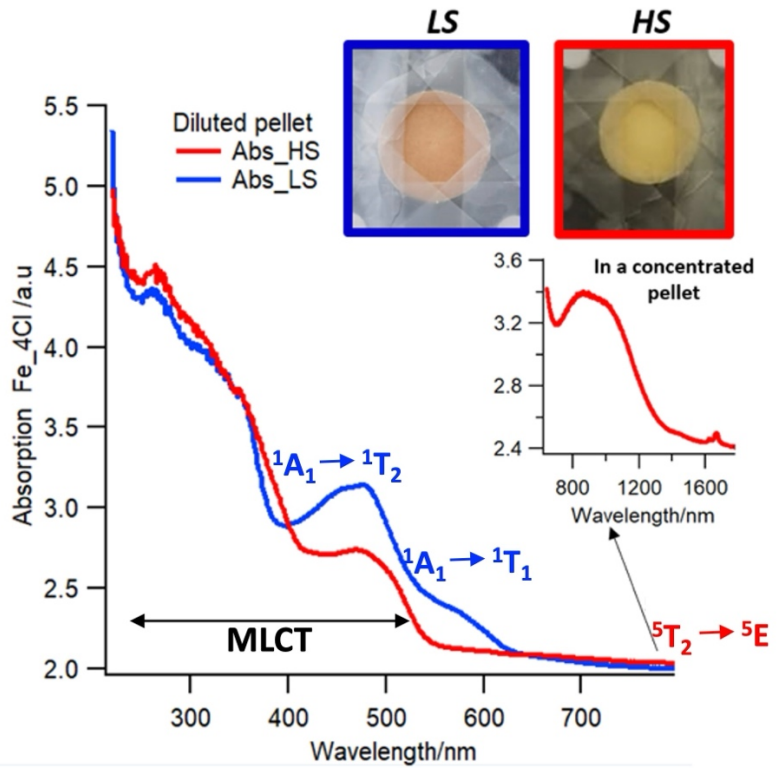

Figure S3. Diffuse reflectance spectra of **4Cl** in the LS and HS states performed in diluted/concentrated KBr pellets. The observed spectra is a combination of MLCT bands superposed essentially with the characteristic LS state d-d bands of the Fe^{II} ion.

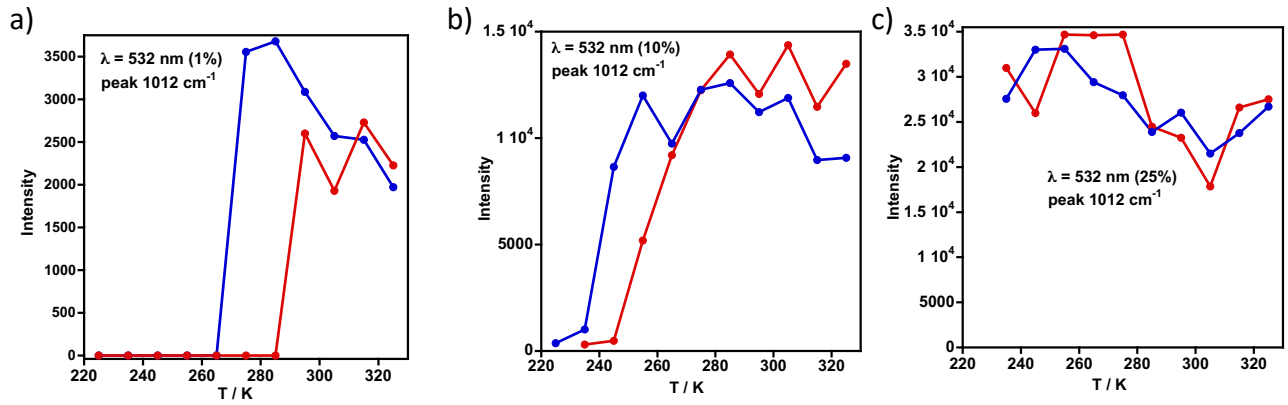

Figure S4. Thermal dependence of the Raman spectrum intensity using a 532 nm laser beam and power 1% (a), 10% (b) and 25% (c) (see text).

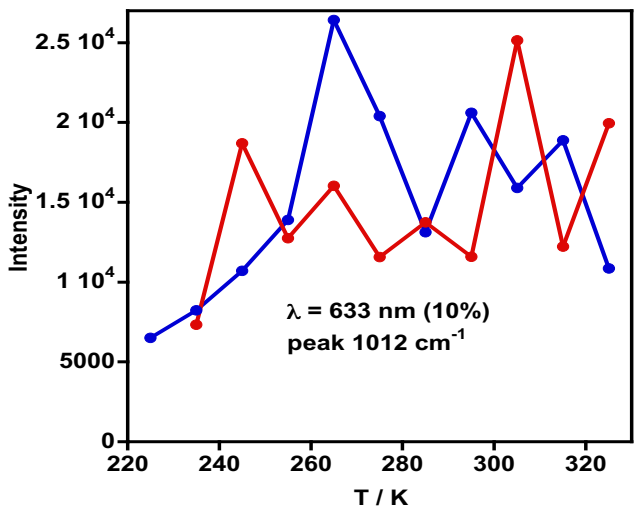

Figure S5. Thermal dependence of the Raman spectrum intensity using a 633 nm laser beam and power 10% (see text).

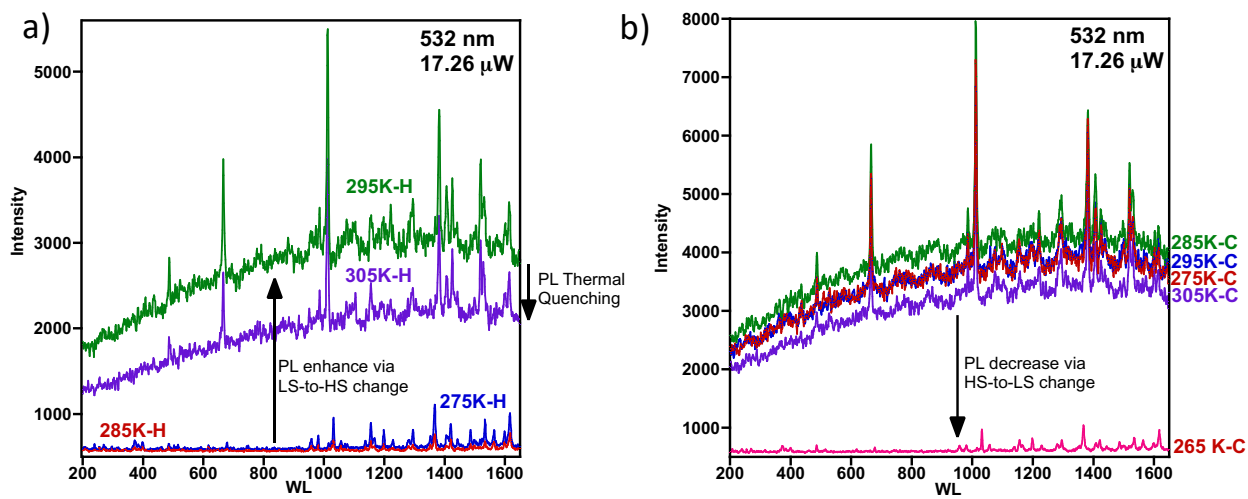

Figure S6. Influence of the photo-luminescence on the base-line of the Raman spectra in the cooling (a) and heating (b) modes.

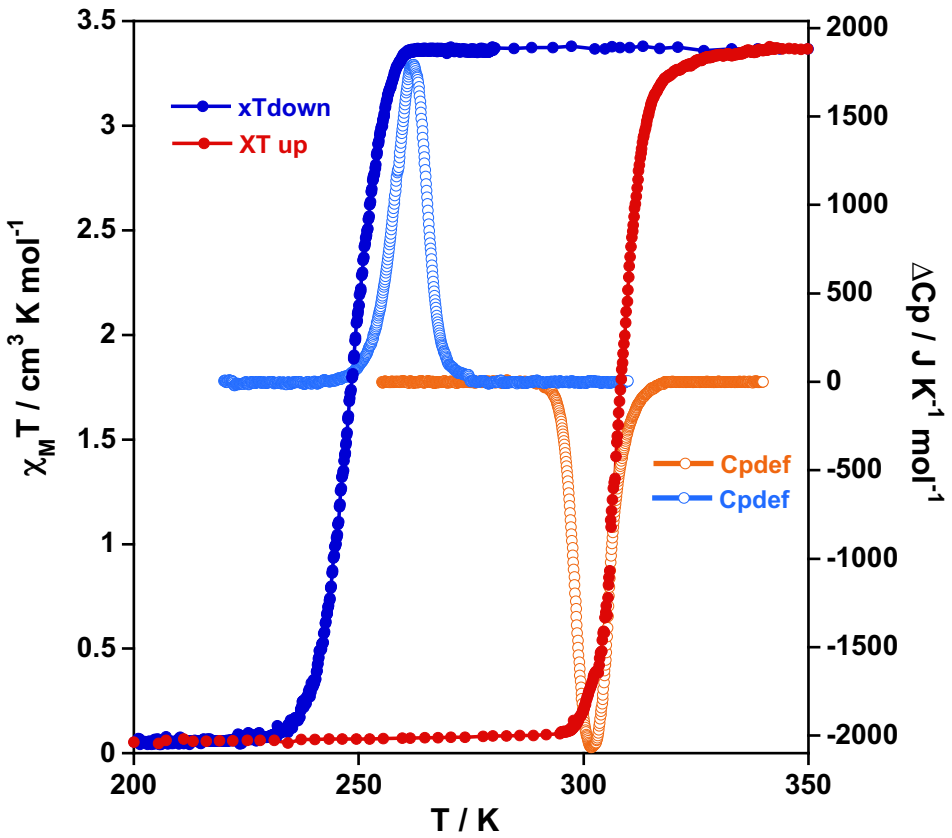

Figure S7. Comparison between $\chi_M T$ and ΔC_p *vs* T for **4Cl**.

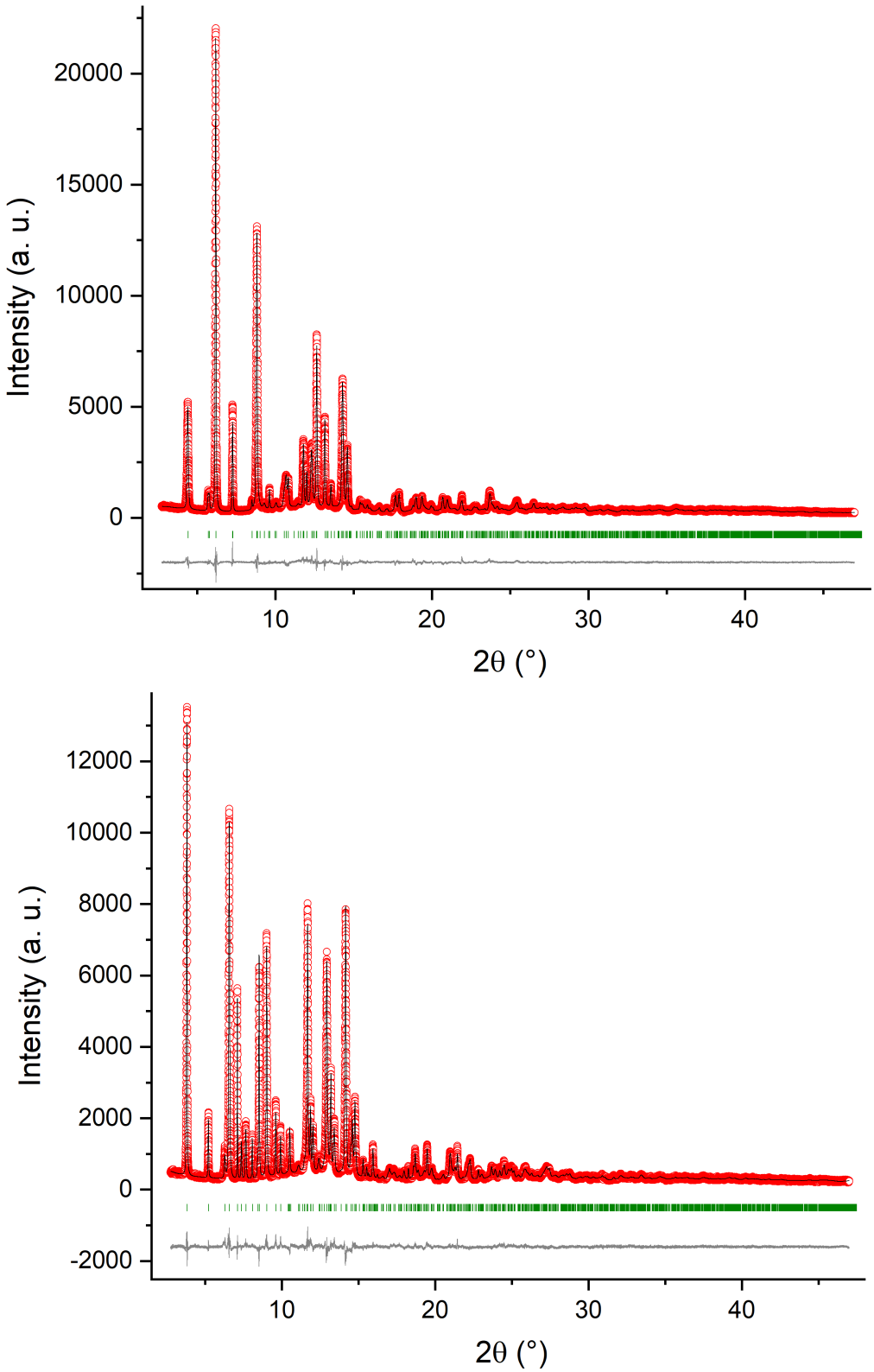

Figure S8. Final Rietveld refinement plots for **4Cl** (LS) (above) and **4Cl** (HS) (below), showing the experimental (red circles), calculated (black line) and difference (grey line) profiles; green marks indicate reflection positions.

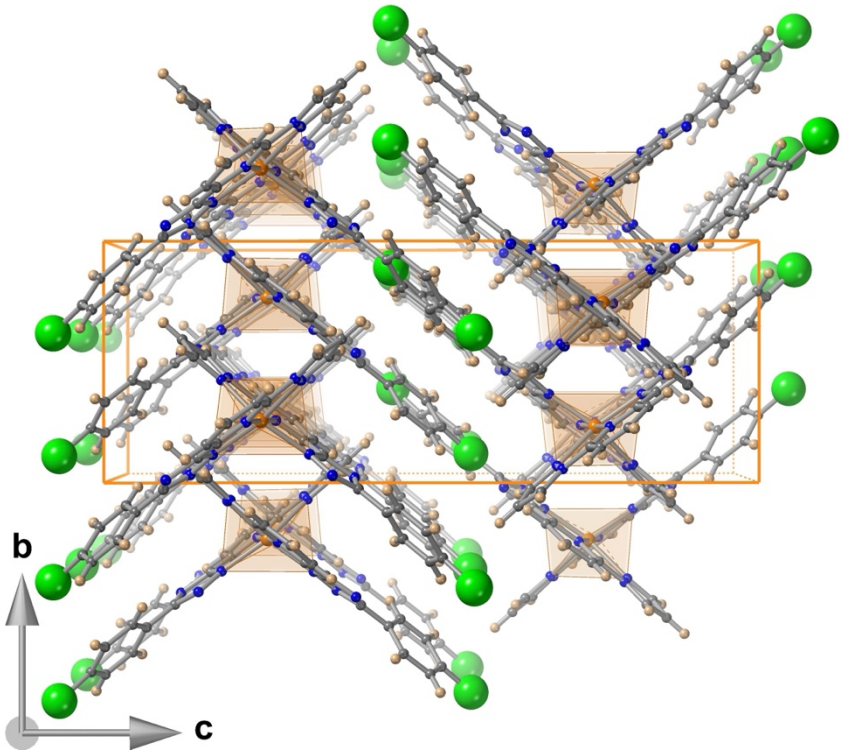

Figure S9. Unit cell of **4Cl** showing the closer stacking along *c* of two adjacent layers laying parallel to the *a*-*b* plane.

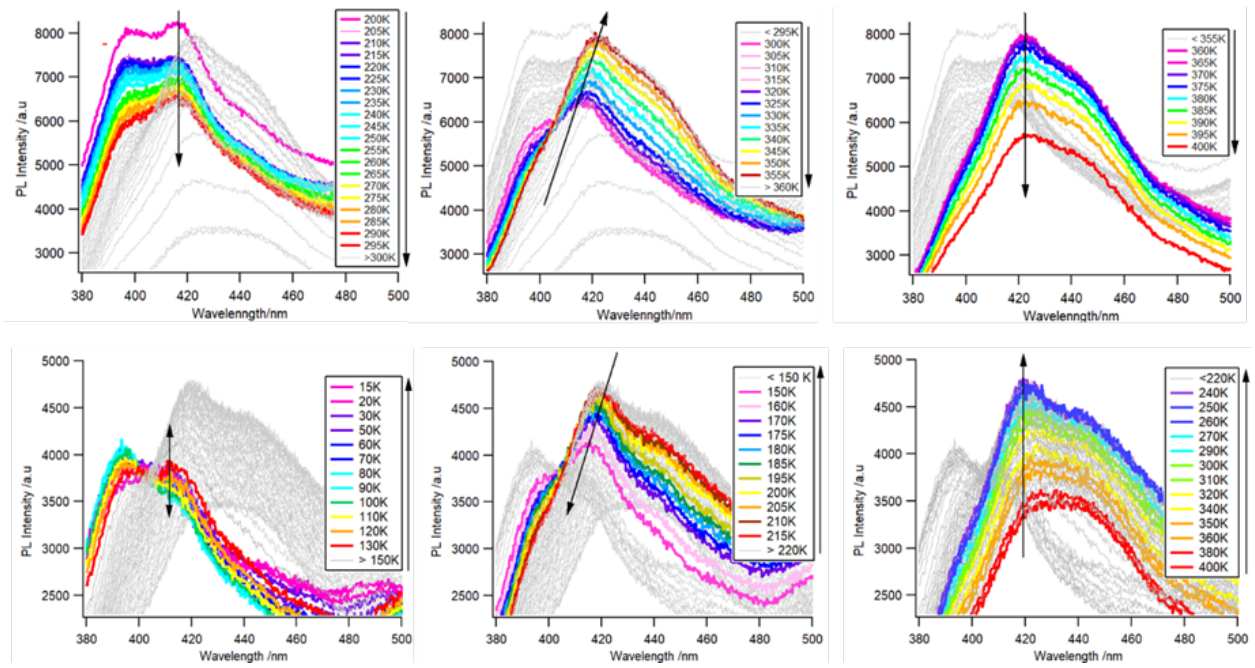

Figure S10. Enlarged representation of the emission thermal spectra dependence for the heating and cooling modes in the 380 - 500 nm interval.